

UC San Diego

UC San Diego Previously Published Works

Title

Relative Effects of Various Factors on Ice Ball Formation and Ablation Zone Size During Ultrasound-Guided Percutaneous Cryoneurolysis: A Laboratory Investigation to Inform Clinical Practice and Future Research

Permalink

<https://escholarship.org/uc/item/8hq803n6>

Journal

Pain and Therapy, 12(3)

ISSN

2193-8237

Authors

Said, Engy T

Marsh-Armstrong, Brennan P

Fischer, Seth J

et al.

Publication Date

2023-06-01

DOI

10.1007/s40122-023-00497-y

Copyright Information

This work is made available under the terms of a Creative Commons Attribution-NonCommercial License, available at <https://creativecommons.org/licenses/by-nc/4.0/>

Peer reviewed



Relative Effects of Various Factors on Ice Ball Formation and Ablation Zone Size During Ultrasound-Guided Percutaneous Cryoneurolysis: A Laboratory Investigation to Inform Clinical Practice and Future Research

Engy T. Said · Brennan P. Marsh-Armstrong · Seth J. Fischer ·
Preetham J. Suresh · Matthew W. Swisher · Andrea M. Trescot ·
J. David Prologo · Baharin Abdullah · Brian M. Ilfeld

Received: February 14, 2023 / Accepted: March 2, 2023 / Published online: March 31, 2023
© The Author(s) 2023

ABSTRACT

Introduction: Ultrasound-guided percutaneous cryoneurolysis provides analgesia using cold temperatures to reversibly ablate peripheral nerves. Cryoneurolysis probes pass a gas through a small internal annulus, rapidly low-

ering the pressure and temperature, forming an ice ball to envelope the target nerve. Analgesia is compromised if a nerve is inadequately frozen, and laboratory studies suggest that pain may be paradoxically induced with a magnitude and duration in proportion with the incomplete ablation. We therefore investigated the relative effects of various factors that may contribute to the size of the ice ball and the effective cryoneurolysis zone.

Methods: A cryoprobe was inserted into a piece of meat, a gas was passed through for 2 min, and the resulting ice ball width (cross-section) and length (axis parallel to the probe) were measured using ultrasound, with the temperature evaluated in nine concentric locations concurrently.

Results: The factor with the greatest influence on ice ball size was probe gauge: in all probe types, a change from 18 to 14 increased ice ball width, length, and volume by up to 70%, 113%, and 512% respectively, with minimum internal temperature decreasing as much as from -5 to -32 °C. In contrast, alternating the type of meat (chicken, beef, pork) and the shape of the probe tip (straight, coudé) affected ice ball dimensions to a negligible degree. The ice ball dimensions and the zone of adequate temperature drop were not always correlated, and, even within a visualized ice ball, the temperature was often inadequate to induce Wallerian degeneration.

Supplementary Information The online version contains supplementary material available at <https://doi.org/10.1007/s40122-023-00497-y>.

E. T. Said · S. J. Fischer · P. J. Suresh ·
M. W. Swisher · B. Abdullah · B. M. Ilfeld (✉)
Department of Anesthesiology, University of
California San Diego, 9500 Gilman Drive, MC 0898,
La Jolla, CA 92093-0898, USA
e-mail: bilfeld@health.ucsd.edu

B. P. Marsh-Armstrong
Department of Medicine, University of California
San Diego, La Jolla, CA, USA

A. M. Trescot
Florida Pain Relief Group, Tampa, FL, USA

J. D. Prologo
Department of Radiology, Emory University,
Atlanta, GA, USA

M. W. Swisher · B. M. Ilfeld
Outcomes Research Consortium, Cleveland, OH,
USA

Conclusions: Percutaneous probe design can significantly influence the effective cryoneurolysis zone; visualizing a nerve fully encompassed in an ice ball does not guarantee adequate treatment to induce the desired Wallerian degeneration because ice forms at temperatures between 0 and -20°C , whereas only temperatures below -20°C induce Wallerian degeneration. The correlation between temperatures in isolated pieces of meat and perfused human tissue remains unknown, and further research to evaluate these findings in situ appears highly warranted.

Keywords: Analgesia; Postoperative pain; Chronic pain; Acute pain; Cryoneurolysis; Cryoablation

Key Summary Points

Why carry out this study?

Ultrasound-guided percutaneous cryoneurolysis provides analgesia using cold temperatures to reversibly ablate peripheral nerves.

However, analgesia is compromised if a nerve is inadequately frozen, and laboratory studies suggest that pain may be paradoxically induced with a magnitude and duration in proportion with the incomplete ablation.

We therefore investigated the relative effects of various factors that may contribute to the size of the ice ball and effective cryoneurolysis zone.

What was learned from the study?

The factor with the greatest influence on ice ball size was probe gauge, while alternating the type of meat and the shape of the probe tip affected ice ball dimensions to a negligible degree.

Ice ball dimensions and the zone of adequate temperature drop were not always correlated, and, even within a visualized ice ball, the temperature was often inadequate to induce Wallerian degeneration.

Percutaneous probe design can significantly influence the effective cryoneurolysis zone; visualizing a nerve fully encompassed in an ice ball does not guarantee adequate treatment to induce the desired Wallerian degeneration.

INTRODUCTION

Cryoneurolysis is an analgesic modality cleared by the United States Food and Drug Administration to treat both acute and chronic pain; in cryoneurolysis, extremely cold temperatures reversibly ablate peripheral nerves via the induction of Wallerian degeneration [1]. Historically, a surgically exposed nerve would be treated under direct vision, but the development of percutaneous probes in the 1980s and the more-recent proliferation of ultrasound imaging technology have allowed for widespread non-operative bedside cryoneurolysis. The confluence of these three modalities—small cryoneurolysis machines, percutaneous probes, and portable ultrasound units—has increased interest in using cryoneurolysis to treat both postoperative [2–4] and chronic [5, 6] pain.

Modern cryoneurolysis probes pass a gas—typically nitrous oxide or carbon dioxide—down their length and through a small internal annulus, which lowers the pressure and results in a rapid temperature decrease due to the Joule–Thomson effect. The decreased temperature induces an ice ball to form on the outside of the probe (the gas is vented back out via the probe). Axons exposed to temperatures between -20 and -100°C undergo Wallerian degeneration and then regrow at approximately 2 mm/day, resulting in a reversible and variable

sensory and motor block with a duration lasting weeks to months [7, 8]. Therefore, the part of the ice ball between -20 and -100 °C is the “zone of effectiveness.” Since the ice ball is hypoechoic on ultrasound [9], providers use ultrasound visualization as a proxy to identify the zone of therapeutic freezing and attempt to encompass the target nerve within the ice ball’s border [10]. The larger the ice ball, the larger the presumed zone of adequate treatment [11, 12]. Unfortunately, a temperature in the range of 0 to -20 °C will produce an ice ball but also an unpredictable and short-duration neuropraxia instead of the desired long-term analgesia resulting from Wallerian degeneration [13].

Prior studies have demonstrated that if a nerve is *inadequately* frozen, a paradoxical response can occur, inducing several weeks of hyperalgesia with a magnitude and duration in proportion with the incomplete ablation [14]. Consequently, maximizing the ice ball zone of effectiveness is of paramount importance, possibly marking the difference between success—inducing complete axonotmesis and providing analgesia for weeks or months [2]—and failure: producing a neuropraxia and possibly inducing pain [13].

Multiple factors that influence ice ball size have been identified, such as tissue osmolality and cryoprobe temperature [15]. However, more recently designed percutaneous-specific probes are designed to increase ice ball size. While theoretically beneficial, their relative effects remain unknown. We therefore investigated the relative effects of various factors that may contribute to the size of the effective cryoneurolysis zone. Our objective was to inform both clinical practice and future laboratory research.

METHODS

This laboratory study did not involve live animals and, therefore, no Institutional Animal Care and Use Committee (IACUC) oversight was sought or required. Pieces of chicken breast, pork loin, and beef filets (5–8 cm in thickness) were heated to 20 °C (37 °C for one experiment) in water baths (Fig. 1A) using heating units (Culinary Sous Vide Precision Cooker Pro, 1200 W, San Francisco, CA).

The nine temperature probes were calibrated prior to data collection until they could each perform three consecutive readings that were all within 0.5 °C of three known-temperature standards: dry ice (-78.5 °C), an ice bath (0 °C), and the 37 °C water bath (Digi-Sense Traceable Memory-Loc Datalogging Thermometer, Cole-Parmer Instrument Company, Vernon Hills, IL). The internal tissue temperature was confirmed to match the water bath temperature prior to experimentation.

Cryoneurolysis procedures were executed in an identical heated water bath setup with a single piece of meat placed on a submerged “stand” created specifically for this project from ABS plaster with a layer height of 0.1 mm and hole tolerances of 0.3 mm (Ultimaker S5, Herndon Corp., Herndon, Virginia). The stand included a single hole for the cryoneurolysis probe which kept the probe at a 30° angle of approach, allowing the depth required for the ice ball to form while at the same time allowing measurement of the cross-sectional area of the

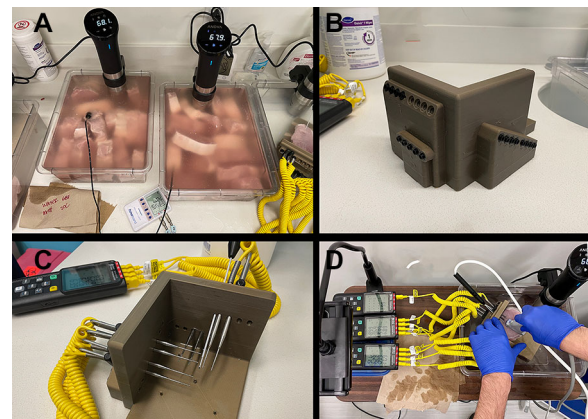


Fig. 1 Equipment. **A** Pieces of meat heated in a water bath using heating units (Culinary Sous Vide Precision Cooker Pro, 1200 W, San Francisco, CA). **B** A stand to hold the cryoneurolysis probe at a 30° angle of approach and nine tapered thermocouple temperature probes at precise 5-mm increments in all three dimensions relative to the end of the cryoprobe. **C** The stand created with a three-dimensional printer with the temperature probes inserted (Cooper-Atkins 50209-K micro-needle thermocouple type K probe, Cooper-Atkins Corp., Middlefield, CT). **D** Positioning of the equipment during measurements

ice ball (Fig. 1B). Additional holes held nine tapered thermocouple temperature probes (Cooper-Atkins 50209-K micro-needle thermocouple type K probe, Cooper-Atkins Corp., Middlefield, CT) situated along vectors both in and out of plane in 5-mm increments from the middle for the cryoprobe bare-metal tip, the center of ice ball formation (Fig. 1C). This increment size was limited by the ~ 5 mm max. diameter of the temperature probes themselves.

The factors investigated to inform future laboratory research included three types of animal muscle (chicken breast, pork loin, beef filet mignon) as well as muscle temperature (20 vs. 37 °C). In addition, we measured the ice ball cross-sectional diameter at 30-s increments until the maximum diameter was reached using a straight 14-gauge probe with a trocar end and creased annulus (nitrous oxide from an e-cylinder).

The factors investigated to inform clinical practice included various probe characteristics and the type of gas. Larger probes theoretically produce larger ice balls but may be less comfortable for patients due to their larger diameter. We therefore compared a relatively small 18 gauge to a 14 gauge, one of the largest commonly used probes in clinical practice. While probes are traditionally straight along their entire axis, a new “coudé” shape theoretically increases ice ball width, and we therefore compared straight with coudé (Fig. 2A). Probes with a triangular or “trocar” end are designed to improve the ease of passage through tissue, but their effect on ice ball size compared with blunt-end designs remaining unknown, and we thus compared the two types (Fig. 2B). The original annulus design was machined, but a new “creased” annulus purportedly increases the diameter of the ice ball to an unknown degree, so we compared traditional (non-creased) to creased designs (Fig. 2C–F). Lastly, most modern percutaneous cryoprobes utilize either nitrous oxide or carbon dioxide, and we therefore compared the two gasses. Since a connector for carbon dioxide was not available for an e-cylinder, we used 20-pound cylinders for both types of gasses to vary only a single factor for this comparison.

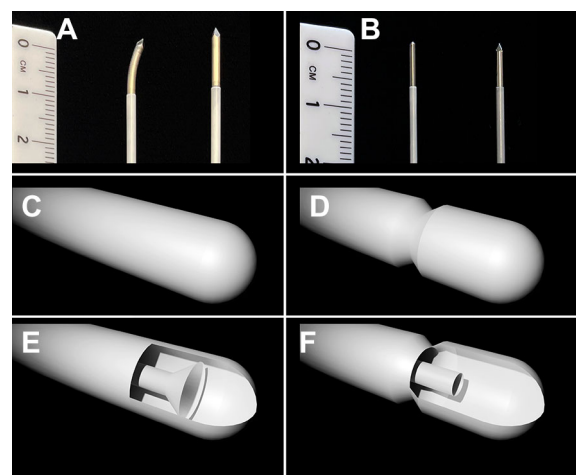


Fig. 2 Probes. **A** A new curved (“coudé”) versus a traditional straight probe. **B** A rounded or “blunt” versus a trocar-tipped probe. **C, D** External rendering of a traditional versus a “creased” probe. **E, F** Internal rendering of the traditional versus creased annulus. Renderings are included to illustrate the relative differences between annulus designs and are not drawn to scale (the renderings were created by Elan F. Ilfeld)

The factors held constant unless specifically being investigated included a medium of pork loin at 20 °C, a probe with a creased annulus and straight trocar end, and nitrous oxide gas from an e-cylinder. A 13- to 6-MHz linear-array ultrasound transducer (HFL38, Edge-II, SonoSite, Bothell, Washington) was placed on the surface of the submerged piece of meat with the cryoprobe (PainBlocker, Epimed International, Dallas, TX), initially in plane (Fig. 1D). The cryoneurolysis machine was activated for 2 min, at which time the ice ball width and length were measured (details below in the “[Outcome measures](#)” section). Temperatures were measured throughout freezing at locations 0, 5, 10, 15, and 20 mm from the cryoprobe tip, both in line with and perpendicular to the probe path (nine temperature probes in total; only one 0-mm probe), and for up to 45 s after freezing concluded. In addition, three trials were performed where we measured the ice ball cross-sectional diameter and temperatures at 30-s increments for 8.5 min and a subsequent 2-min thaw to observe when the maximum diameter was reached (probe: straight, 14-gauge, creased annulus, trocar end, with nitrous oxide from an

e-cylinder). Each piece of meat was disposed of after the trial concluded. For each factor investigated, three trials ($N = 3$) were performed, a unique near-identical piece of meat being used for each. Larger sample sizes were not explored due to both the intent of this study to obtain relativistic rather than absolute metrics and the high repeatability and minimal variability of placing a single cryoprobe into near-identical pieces of meat. As the distribution of data could not be explored for each factor investigated, median metrics were used for all analyses.

Outcome Measures

For each freezing cycle, the cryoneurolysis machine was activated for 2 min with either nitrous oxide or carbon dioxide from an e-cylinder or 20-pound cylinder, at which time the width (the widest cross-section perpendicular to the plane of the cryoprobe) and length (parallel to the cryoprobe) of the ice ball were measured, along with temperature readings from all thermocouple probes (Fig. 1D).

While ice ball volume might intuitively seem to be the outcome of greatest interest, in clinical practice, a nerve cannot be positioned in the center of the elongated sphere—called a “prolate spheroid” (similar in shape to a rugby ball)—since the probe itself comprises the central axis. In clinical use, the end of the probe is usually placed adjacent to the target nerve, and therefore the most relevant dimension is often the distance between the side of the probe and the border of the ice ball in the maximum cross-section plane of the prolate spheroid. This specific distance cannot be accurately measured using ultrasound because the surface of the ice ball has an impedance that results in an acoustic shadow that completely obscures the probe itself. Consequently, we used the maximum width of each ice ball as a primary outcome and retained the length and volume as secondary outcomes, since they do influence the zone of treatment. While ice ball width and length were measured directly, the volume in cubic millimeters was calculated using the prolate spheroid formula: $4.19 \times (\text{width}/2)^2 \times (\text{length}/2)$.

Regarding the ice ball temperature, time-dependent temperature–location data (nine data points reported every 10 s) were projected into three-dimensional space with a Y dimension of temperature and were fitted to a three-dimensional Gaussian with two degrees of freedom.¹ This fit was used to generate a time-dependent estimated heatmap of temperatures along the XZ plane relative to the probe and a central temperature versus time graph for each trial. This was done using a custom Python script (Python Software Foundation, Wilmington, DE).

RESULTS

Factors to Inform Laboratory Research

During the 8.5-min continuous freeze (Fig. 3), the probe tip reached -20°C after 30 s, and by 2 min it had reached -30.6°C , which was approximately 90% of the lowest temperature (-33.7°C) recorded at the end of the 8.5-min freeze cycle. The ice ball width (cross-section perpendicular to the probe) after 2 min of freeze was 11.5 mm, which was 65% of the 17.8-mm maximum occurring at 8 min (Fig. 3). Following the cessation of gas activation, the width of the ice ball diminished by only 6% in the following 2 min of thaw, while the temperature took less than 20 s to fall below the -20°C threshold required to produce Wallerian degeneration (Fig. 3). Increasing the pork loin temperature from 20 to 37°C decreased the ice ball width by 13% and the length 28% (Table 1) and changed the lowest temperature achieved at 2 min from -32 to only -15°C (Fig. 4). While all three types of meat resulted in similar ice ball dimensions (Table 1), the lowest temperature recorded varied: -28°C for beef, -32°C for pork, and -38°C for chicken (Fig. 5).

$$^1 Y = O - Ae^{-\left(a(X-X_0)^2 + b(X-X_0)(Z-Z_0) + c(Z-Z_0)^2\right)}, \quad a = \frac{\cos^2(\theta)}{2\sigma_x^2} + \frac{\sin^2(\theta)}{2\sigma_z^2}, \quad b = \frac{-\sin^2(2\theta)}{4\sigma_x^2} + \frac{\sin^2(2\theta)}{4\sigma_z^2}, \quad c = \frac{\sin^2(\theta)}{2\sigma_x^2} + \frac{\sin^2(2\theta)}{2\sigma_z^2}.$$

Input data: Y = temperature, X , Z = location. Fitted parameters: O = offset; A = amplitude; X_0 , Z_0 = center location, σ = standard deviation; θ = fitting parameter.

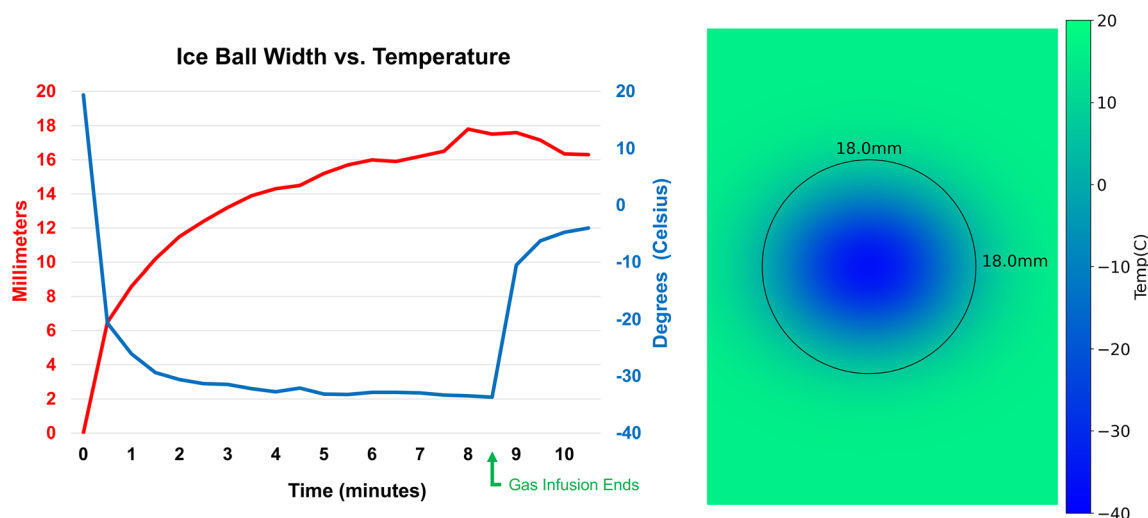


Fig. 3 Ice ball dimensions and temperature with 8.5 continuous minutes of nitrous oxide from an e-cylinder through a 14-gauge, creased-annulus, trocar-tipped probe in a pork loin starting at a 20 °C baseline (PainBlocker, Epimed International, Dallas, TX). The visible ice ball width and length were determined at 30-s intervals using ultrasound, and the maximum dimensions are represented by the *black circle in the right-hand panel*. Concurrent temperature readings recorded at 10-s intervals using multiple thermocouples at 5-mm increments in all three dimensions are represented by the *green and blue heatmap*

(Cooper-Atkins 50209-K micro-needle thermocouple type K probe, Cooper-Atkins Corp., Middlefield, CT). The *y*-axis values of the graph are the medians of three separate measurements at each time point, while the heatmap was created from the first measurement only due to the quantity of data collected. Therefore, dimensions may vary between the graph and heatmap by 1–2 mm. The graph data should be viewed as the most accurate regarding specific ice ball dimensions, while the heatmap provides an overall idea of the heat distribution

Factors to Inform Clinical Care and Laboratory Research

Altering the end of the probe from the traditional straight to a new curved “coudé” shape (Fig. 2A) changed the ice ball minimum temperature or dimensions to a negligible degree (Table 1). In contrast, the factor with the greatest influence was probe gauge: changing it from 18 to 14 increased ice ball width, length, and volume by 70%, 113%, and 512%, respectively (Table 1). Perhaps even more importantly, in contrast to the 14-gauge probes, no 18-gauge instrument reduced the temperature below the -20 °C threshold required to induce Wallerian degeneration (Fig. 6).

The new “creased” annulus design (Fig. 2C–F) did increase the ice ball dimensions, but far more so with a 14-gauge relative to an 18-gauge probe (Table 1). Curiously, while adding the creased design decreased the

minimum ice ball temperature for the 14-gauge probe, it had the opposite effect with the 18-gauge probe. Switching from a blunt/rounded to a trocar end (Fig. 2B) both increased the ice ball dimensions (Table 1) and lowered the minimum ice ball temperature (Fig. 6). Finally, when using 20-pound cylinders, switching from nitrous oxide to carbon dioxide increased the ice ball dimensions (Table 1) but raised the minimum ice ball temperature (Fig. 7).

Data Reliability

All temperature probes met the initial calibration criteria described above. In all trials except the 8.5-min continuous freeze, where larger areas of the tissue were cooled, the 20-mm-from-center temperature reading stayed nearly constant, with an average intra-trial range of 0.4 ± 0.1 °C across all study arms ($N = 13$), both

Table 1 Factors and ice ball dimensions as well as minimum temperatures

Factor	Temp	Muscle	Shape	Crease	Gauge	End	Gas	Lowest ice temp	Width		Length		Volume		
									mm	Change	mm	Change	mm ³	Change	
Temperature	37°C	Pork	Straight	Yes	14	Trocar	N ₂ O	-15 °C	9.8	14%	10.8	40%	543	83%	
	20°C							-32 °C	11.2		15.1		991		
Medium	20°C	Beef	Straight	Yes	14	Trocar	N ₂ O	-28 °C	11.2	0%	16.0	0%	1050	0%	
		Chicken						-38 °C	11.2		16.0		1050		
		Pork						-32 °C	11.2		0%		15.1		-6%
Shape	20°C	Pork	Coude	Yes	14	Trocar	N ₂ O	-29 °C	11.1	1%	14.7	3%	948	4%	
			Straight					-32 °C	11.2		15.1		991		
Crease	20°C	Pork	Straight	No	14	Trocar	N ₂ O	-14 °C	9.7	15%	9.6	57%	473	110%	
				Yes				-32 °C	11.2		15.1		991		
				No	18			-16 °C	6.2	6%	5.9	20%	119	36%	
				Yes				-5 °C	6.6		7.1		162		
Gauge	20°C	Pork	Straight	No	18	Trocar	N ₂ O	-16 °C	6.2	56%	5.9	63%	119	298%	
				Yes	14			-14 °C	9.7		9.6		473		
				Yes	18			-5 °C	6.6	70%	7.1	113%	162	512%	
					14			-32 °C	11.2		15.1		991		
					18			Blunt	-12 °C	7.6	36%	8.6	9%	260	101%
					14				-18 °C	10.3		9.4		522	
End	20°C	Pork	Straight	Yes	14	Blunt	N ₂ O	-18 °C	10.3	9%	9.4	61%	522	90%	
						Trocar		-32 °C	11.2		15.1		991		
Gas *	20°C	Pork	Straight	Yes	14	Trocar	N ₂ O	-33 °C	7.7	12%	10.0	14%	310	42%	
							CO ₂	-24 °C	8.6		11.4		441		

The lowest temperatures at the tip of the probes are presented, with minimum temperatures higher than -20 °C denoted in red

While ice ball width, length, and temperature were measured directly, the volume in cubic millimeters was calculated using the prolate spheroid formula: $4.19 \times (\text{width}/2)^2 \times (\text{length}/2)$. Each ice ball dimension is the median of three separate measurements, while the heatmaps of the static figures and supplemental graphics interchange format figures were drawn from the first measurement only due to the quantity of data collected. Therefore, dimensions among the table, graphs, and heatmaps may vary by 1–2 mm. The table and figure data should be viewed as the most accurate regarding specific ice ball dimensions, while the heatmaps provide an overall idea of the heat distribution

*An e-cylinder was used for all experiments with the exception of nitrous oxide versus carbon dioxide in which a 20-pound cylinder was used for both

indicating stable ambient tissue temperatures and giving an approximate expected error in the temperatures reported above. At all recorded timepoints, at all locations, and in all trials where a temperature heatmap was calculated, residual values between the modeled temperature and measured temperature did not exceed 2 °C. While not enough trials ($N = 3$) per variable were conducted to ensure the normal distribution requisite to reporting means or standard errors of ice ball dimensional data, if a normal distribution is assumed and standard

error values are propagated through subsequent calculations, the percent differences for length and width reported above have, at most, 1.5% standard errors. The propagated standard error for the percent difference in volume reported above is ~ 10.9%. In all cases, the temperatures and percent differences reported within the “Results” section are, respectively, distinct from each other and from zero by more than these speculative standard errors.

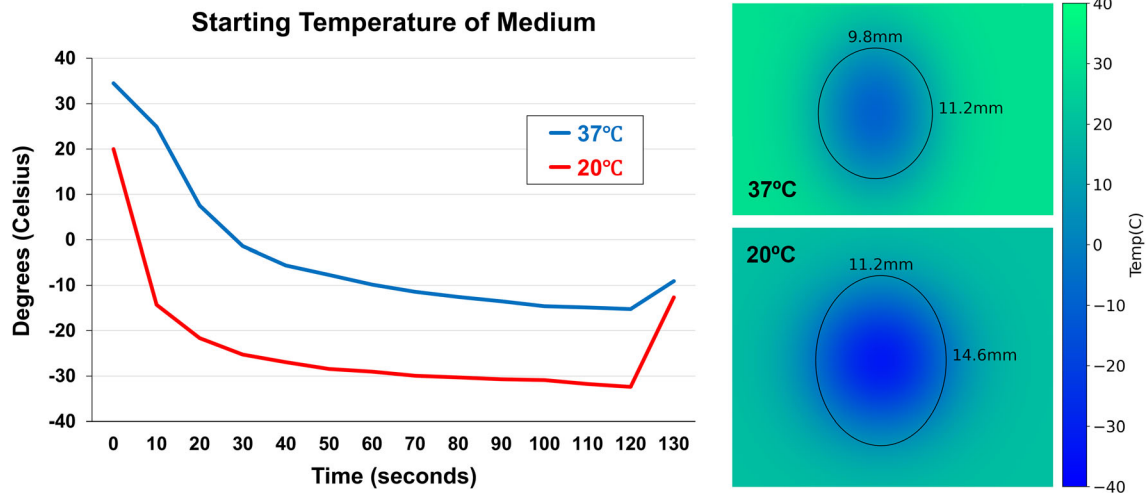


Fig. 4 Effects of baseline temperature on ice ball dimensions and temperature with 2 min of nitrous oxide from an e-cylinder through a 14-gauge, creased-annulus, trocar-tipped probe in pork loin (PainBlocker, Epimed International, Dallas, TX). The visible ice ball width and length were determined at 120 s using ultrasound and are represented by the *black circles in the right-hand panels*.

Concurrent temperature readings recorded at 10-s intervals using multiple thermocouples at 5-mm increments in all three dimensions are represented by the *green and blue heatmap* (Cooper-Atkins 50209-K micro-needle thermocouple type K probe, Cooper-Atkins Corp., Middlefield, CT)

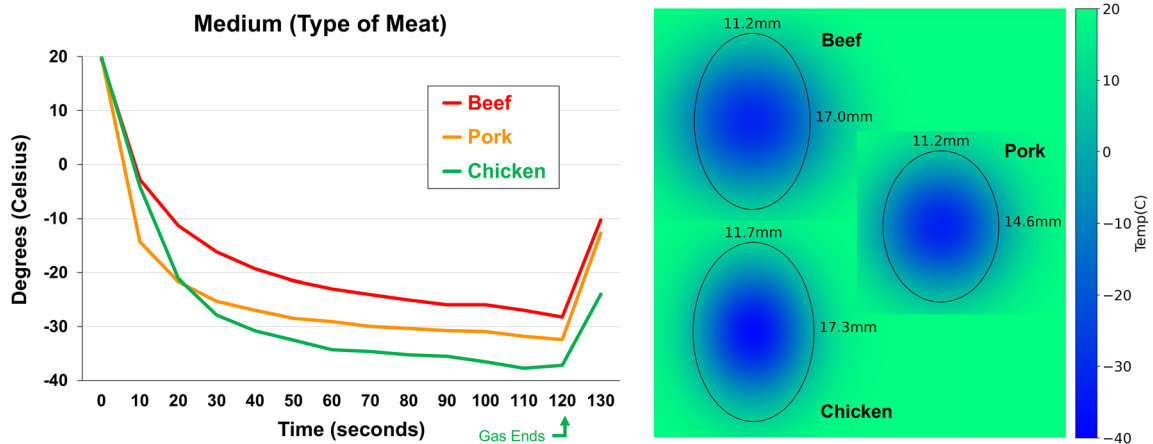


Fig. 5 Effects of different media on ice ball dimensions and temperature with 2 min of nitrous oxide from an e-cylinder through a 14-gauge, creased-annulus, trocar-tipped probe in meat starting at a 20 °C baseline (PainBlocker, Epimed International, Dallas, TX). The visible ice ball width and length were determined at 120 s using ultrasound and are represented by the *black circles in*

the right-hand panels. Concurrent temperature readings recorded at 10-s intervals using multiple thermocouples at 5 mm increments in all three dimensions are represented by the *green and blue heatmap* (Cooper-Atkins 50209-K micro-needle thermocouple type K probe, Cooper-Atkins Corp., Middlefield, CT)

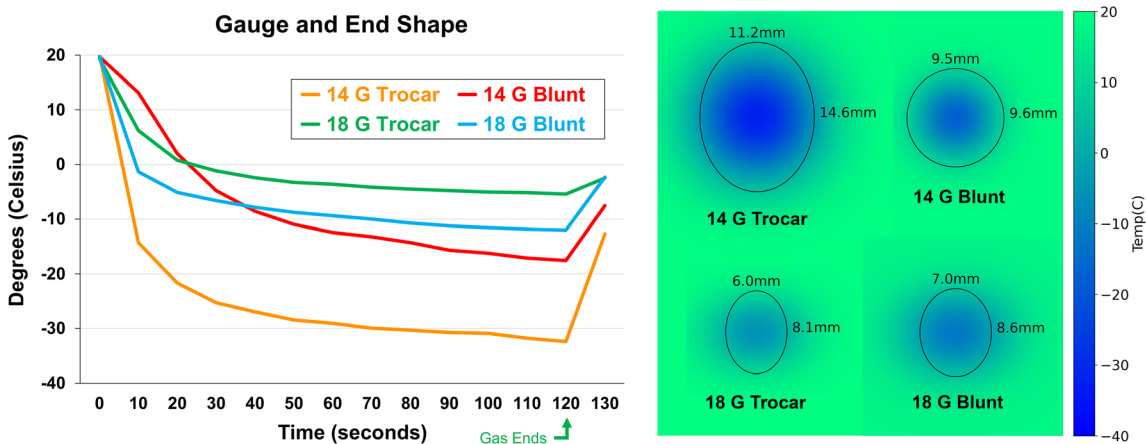


Fig. 6 Effects of probe gauge and distal tip design on ice ball dimensions and temperature with 2 min of nitrous oxide from an e-cylinder through a creased-annulus probe in a pork loin starting at a 20 °C baseline (PainBlocker, Epimed International, Dallas, TX). The visible ice ball width and length were determined at 120 s using ultrasound and are represented by the *black circles in the*

right-hand panels. Concurrent temperature readings recorded at 10-s intervals using multiple thermocouples at 5-mm increments in all three dimensions are represented by the *green and blue heatmap* (Cooper-Atkins 50209-K micro-needle thermocouple type K probe, Cooper-Atkins Corp., Middlefield, CT)

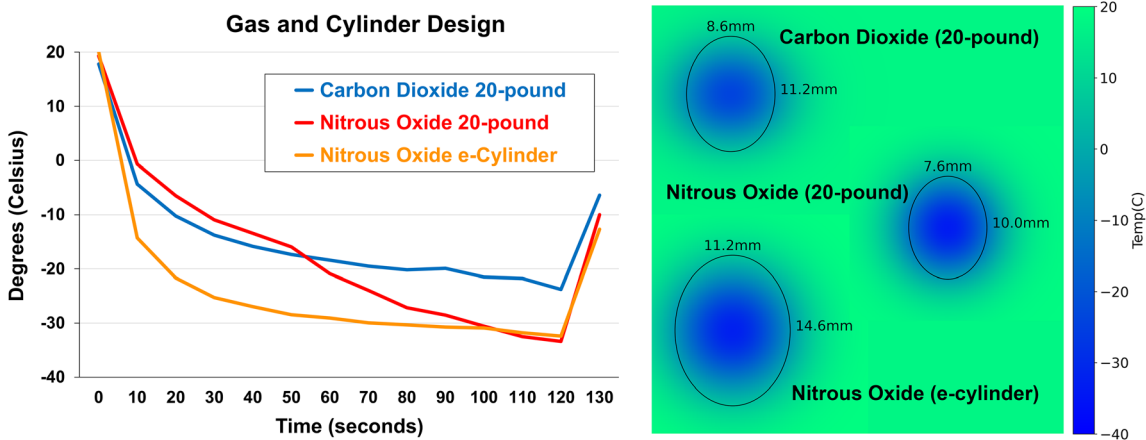


Fig. 7 Effects of gas and cylinder design on ice ball dimensions and temperature with 2 min of gas flow through a creased-annulus probe in a pork loin starting at a 20 °C baseline (PainBlocker, Epimed International, Dallas, TX). The visible ice ball width and length were determined at 120 s using ultrasound and are represented

by the *black circles in the right-hand panels*. Concurrent temperature readings recorded at 10-s intervals using multiple thermocouples at 5-mm increments in all three dimensions are represented by the *green and blue heatmap* (Cooper-Atkins 50209-K micro-needle thermocouple type K probe, Cooper-Atkins Corp., Middlefield, CT)

Dynamic temperature heat maps and core temperature vs. time graphs are provided in the Supplementary Information.

DISCUSSION

This laboratory investigation identified the relative effects of various factors that contribute to

the size of the effective cryoneurolysis zone. Increasing the probe size (lower gauge) produced a larger ice ball and colder temperatures, while the shape of the probe end (e.g., curved vs. straight) had negligible effects. These findings are of paramount importance when choosing a probe for percutaneous cryoneurolysis which relies on lowering the temperature to at least -20°C to induce Wallerian degeneration [2–6]. Since an ice ball forms at temperatures colder than 0°C and is easily viewed by ultrasound, this is used by clinicians as a proxy for the effective zone of cryoneurolysis. However, lowering neural tissue only into the range of 0 to -20°C gives the illusion of effective cryoneurolysis, when, in actuality, a neuropraxia may result. Furthermore, an incomplete cryolesion may induce hyperalgesia lasting several weeks [14] (not to be confused with neuropathic pain lasting multiple months observed in laboratory animals with complete lesions and concurrent nerve manipulation [16–18]).

While it may therefore seem concerning that all 18-gauge probes tested resulted in temperatures in this 0 to -20°C range, the correlation between temperatures in isolated pieces of meat and perfused human tissue remains unknown, necessitating further study. Relatedly, while 14-gauge probes did produce temperatures below -20°C , this was only the case when the pork loin medium started at 20°C . When the pork loin was increased to body temperature (37°C), an inherently more challenging medium to reach therapeutic temperatures in, not only were the ice ball dimensions reduced, but the coldest temperature observed was only -15°C after a clinically typical 2-min freeze, suggesting a sub-therapeutic treatment when used in patients. However, in a randomized, double-masked, sham-controlled trial involving 60 patients undergoing mastectomy [2], smaller 16-gauge probes decreased postoperative pain for up to 1 year, demonstrating clinical effectiveness of ultrasound-guided percutaneous cryoneurolysis with the equipment used in our laboratory study. We used 20°C as the standard baseline meat temperature for all other comparisons because using 37°C cooked the meat,

which could have compromised the experiments.

While including a thermocouple at the probe tip to detect real-time temperature appears advisable—and is available on some models—even that cannot guarantee a therapeutic temperature below -20°C throughout the visualized ice ball, since temperature increases with distance from the end of the probe. The three-dimensional heat maps illustrated this issue: at the periphery of the ultrasound-visualized ice ball, the temperature was greater than -20°C ; the percentage of the ice ball that was subtherapeutic could not be deduced simply from ice ball dimensions. Indeed, a larger ice ball does not necessarily indicate a lower core temperature: carbon dioxide produced an ice ball that had 42% greater volume yet was 9°C warmer than when nitrous oxide was used (-24 vs. -33°C). Conversely, similarly sized ice balls do not necessarily indicate similar core temperatures. At no point in one of the 2-min freezes (the clinical standard) was the temperature below -20°C even 5 mm from the ice ball core in either dimension. Therefore, to maximize the desired Wallerian degeneration, clinicians should place the target nerve as close to the probe tip as possible and not simply within the ice ball's periphery.

Another clinically relevant finding was the dissociation between temperature and ice ball dissolution when the gas infusion stopped. Even after an 8.5-min freeze—a far longer duration than typically used clinically—it required only 15 s for the temperature to increase above -20°C in this non-perfused model, while the ice ball width had not diminished in that period of time, and decreased only 7% (1.2 mm) in the full 2 min following gas flow cessation. The ice ball will resolve far faster in situ with warm blood flow, so, barring future data to the contrary, clinicians should assume that the therapeutic cryoneurolysis period ends as soon as gas flow has concluded, regardless of the ice ball appearance.

Although the new curved “coudé” probe did not produce a wider ice ball overall, the functional width of the ice ball is probably greater when the target nerve is located in the “elbow” or curve of the tip. Unlike a straight probe

which forms the central axis of an ice ball—with 50% of ice ball width available on either side—the curve of the coudé probe is located on the periphery of the ice ball, leaving more width on the concave surface of the probe for the target nerve. Our 3D-printed probe-aligning device could not accommodate the curve of the coudé probe, so generating an accurate heat map was not possible. Additional research is required to fully understand the temperature distribution of this new probe design.

The new “creased” annulus design (Fig. 2C–F) increased the ice ball dimensions and lowered the temperature for the 14-gauge probes. We identified no drawbacks to the new design. It therefore appears to be a beneficial development as compared to the other cryoneurolysis equipment assessed in this study.

Nitrous oxide and carbon dioxide are both commonly used for cryoneurolysis because they become solids at -88 and -78 °C, respectively, which ensures that colder temperatures cannot be reached, which is desirable since permanent tissue destruction occurs at temperatures below -100 °C [1]. It is noteworthy that in our study, nitrous oxide produced a minimum ice ball temperature almost exactly 10 °C lower than carbon dioxide (-33 vs. -24 °C), which appears to be a benefit of the former over the latter. It is also notable that while nitrous oxide from e- and 20-pound cylinders reached approximately the same minimum temperature after 2 min (-32 to -33 °C), the e-cylinder reached -20 °C after approximately 15 s, while it required a full minute to reach this threshold using a 20-pound cylinder. In clinical use, this would result in the temperature required for Wallerian degeneration being applied to the target nerve for nearly twice as long with an e-cylinder. Additionally, the ice ball dimensions were larger when using an e-cylinder, increasing width and length by 45% and 51%, respectively.

This study’s greatest limitation was the use of pieces of tissue heated to a specific sub-homeostatic temperature as a surrogate for the human body. Since our medium did not have a circulation, we did not provide a thaw followed by a repeat of the freeze period, which is

common in clinical use. More importantly, we can make no assertion that this model approximates clinical conditions under which cryoprobes would be used, where tissue is perfused and at physiologic temperature. If anything, this model is less able to dissipate cooling, more favoring larger and colder ice ball formation. So, any probes unable to achieve core temperatures under -20 °C are more unlikely to achieve Wallerian degeneration in situ. Temperature and dimension metrics reported herein cannot be treated as the absolute values that the studied cryoprobes can be expected to achieve during clinical use. The reported values should be considered in terms of what they suggest about the associated probes’ abilities to achieve therapeutic levels of freezing relative to each other.

CONCLUSIONS

This laboratory investigation identified gauge as the probe factor with the largest effect on ice ball size and cryoneurolysis effectiveness zone, demonstrated that ice ball size and effectiveness zone are not always correlated, and suggests that the temperature—even that within a visualized ice ball—may be subtherapeutic. Further, the study revealed that the temperature rises dramatically upon gas flow cessation—far faster than the dissolution of the visible ice ball—and provides evidence to support the clinical use of a new annulus design, trocar probe tip, and nitrous oxide from an e-cylinder. Further research to evaluate these findings in situ appears highly warranted.

ACKNOWLEDGEMENTS

The authors are grateful for the three-dimensional renderings in Fig. 2C–F created by Elan F. Ilfeld.

Funding. Epimed International (Dallas, TX) provided unrestricted research funding and the cryoneurolysis equipment used in this study.

Opinions, interpretations, conclusions, and recommendations are those of the authors and are not necessarily endorsed by this company. Of note, this was an investigator-initiated project and the first author retained complete control of the study protocol; data collection, analysis, and interpretation; and the resulting manuscript. Epimed International was provided with the initial protocol on which to comment; some suggested revisions were incorporated into the protocol while others were not prior to the execution of the study experiments. Following data analysis, the manuscript was made available to this company prior to submission for informational purposes only. No funding or sponsorship was received for this study or the publication of this article.

Author Contributions. All authors assisted in protocol development and manuscript preparation and approved the final manuscript. All authors based in San Diego assisted in executing the experiments and data collection.

Disclosures. Drs. Said, Swisher, Abdullah and Ilfeld: the authors' institution has received funding from Epimed International (Dallas, TX) for other research studies. The institution has also received funding and/or products for other research from SPR Therapeutics (Cleveland, OH), Infutronix (Natick, MA), Masimo (Irvine, CA), and Avanos (Irvine, CA). Dr. Trescot has served on an advisory board for Atricure, (Mason, OH) and is the Chief Medical Officer for Stimwave Technologies (Pompano, FL). Dr. Prologo is the Chief Medical Officer and cofounder of Focused Cryo, Inc. (Atlanta, GA). The remaining authors (Marsh-Armstrong, Fischer and Suresh) report no competing interests.

Compliance with Ethics Guidelines. This laboratory study did not involve live animals and therefore no Institutional Animal Care and Use Committee (IACUC) oversight was sought or required.

Data Availability. The datasets generated during and/or analyzed during the current study are available from the corresponding author on reasonable request. Data will be

shared for collaborative analyses on request to Brian M. Ilfeld (email: bilfeld@health.ucsd.edu) shortly after publication. A data-sharing contract will be required.

Open Access. This article is licensed under a Creative Commons Attribution-NonCommercial 4.0 International License, which permits any non-commercial use, sharing, adaptation, distribution and reproduction in any medium or format, as long as you give appropriate credit to the original author(s) and the source, provide a link to the Creative Commons licence, and indicate if changes were made. The images or other third party material in this article are included in the article's Creative Commons licence, unless indicated otherwise in a credit line to the material. If material is not included in the article's Creative Commons licence and your intended use is not permitted by statutory regulation or exceeds the permitted use, you will need to obtain permission directly from the copyright holder. To view a copy of this licence, visit <http://creativecommons.org/licenses/by-nc/4.0/>.

REFERENCES

1. Ilfeld BM, Finneran JJ. Cryoneurolysis and percutaneous peripheral nerve stimulation to treat acute pain. *Anesthesiology*. 2020;133:1127–49.
2. Ilfeld BM, Finneran JJ, Swisher MW, Said ET, Gabriel RA, Sztain JF, Khatibi B, Armani A, Trescot A, Donohue MC, Schaar A, Wallace AM. Preoperative ultrasound-guided percutaneous cryoneurolysis for the treatment of pain after mastectomy: a randomized, participant- and observer-masked, sham-controlled study. *Anesthesiology*. 2022;137:529–42.
3. Finneran JJ IV, Schaar AN, Swisher MW, Godat LN, Lee JG, Higginson SM, Ilfeld BM. Percutaneous cryoneurolysis of the lateral femoral cutaneous nerve for analgesia following skin grafting: a randomized, controlled pilot study. *Reg Anesth Pain Med*. 2022;47:60–1.
4. Swisher MW, Ball ST, Gonzales FB, Cidambi KR, Trescot AM, Ilfeld BM. A randomized controlled pilot study using ultrasound-guided percutaneous cryoneurolysis of the infrapatellar branch of the saphenous nerve for analgesia following total knee arthroplasty. *Pain Ther*. 2022;11:1299–307.

5. Radnovich R, Scott D, Patel AT, Olson R, Dasa V, Segal N, Lane NE, Shrock K, Naranjo J, Darr K, Surowitz R, Choo J, Valadie A, Harrell R, Wei N, Metyas S. Cryoneurolysis to treat the pain and symptoms of knee osteoarthritis: a multicenter, randomized, double-blind, sham-controlled trial. *Osteoarthritis Cartilage*. 2017;25:1247–56.
6. Kvarstein G, Hogstrom H, Allen SM, Rosland JH. Cryoneurolysis for cervicogenic headache—a double blinded randomized controlled study. *Scand J Pain*. 2019;20:39–50.
7. Trojaborg W. Rate of recovery in motor and sensory fibres of the radial nerve: clinical and electrophysiological aspects. *J Neurol Neurosurg Psychiatry*. 1970;33:625–38.
8. Gaster RN, Davidson TM, Rand RW, Fonkalsrud EW. Comparison of nerve regeneration rates following controlled freezing or crushing. *Arch Surg*. 1971;103:378–83.
9. Kastler A, Gruber H, Gizewski E, Loizides A. Ultrasound assessment of ice-ball formation by cryoneurolysis device in an ex vivo model. *Reg Anesth Pain Med*. 2018;43:631–3.
10. Rhame EE, Debonet AF, Simopoulos TT. Ultrasonographic guidance and characterization of cryoanalgesic lesions in treating a case of refractory sural neuroma. *Case Rep Anesthesiol*. 2011;2011:691478.
11. Littrup PJ, Mody A, Sparschu R, Prchevski P, Montie J, Zingas AP, Grignon D. Prostatic cryotherapy: ultrasonographic and pathologic correlation in the canine model. *Urology*. 1994;44:175–83 (**discussion 183-184**).
12. Weber SM, Lee FT Jr, Warner TF, Chosy SG, Mahvi DM. Hepatic cryoablation: US monitoring of extent of necrosis in normal pig liver. *Radiology*. 1998;207:73–7.
13. Sunderland S. A classification of peripheral nerve injuries producing loss of function. *Brain*. 1951;74:491–516.
14. Myers RR, Heckman HM, Powell HC. Axonal viability and the persistence of thermal hyperalgesia after partial freeze lesions of nerve. *J Neurol Sci*. 1996;139:28–38.
15. Gill W, Da Costa J, Fraser J. The control and predictability of a cryolesion. *Cryobiology*. 1970;6:347–53.
16. DeLeo JA, Coombs DW, Willenbring S, Colburn RW, Fromm C, Wagner R, Twitchell BB. Characterization of a neuropathic pain model: sciatic cryoneurolysis in the rat. *Pain*. 1994;56:9–16.
17. Wagner R, DeLeo JA, Heckman HM, Myers RR. Peripheral nerve pathology following sciatic cryoneurolysis: relationship to neuropathic behaviors in the rat. *Exp Neurol*. 1995;133:256–64.
18. Wagner R, DeLeo JA, Coombs DW, Myers RR. Gender differences in autotomy following sciatic cryoneurolysis in the rat. *Physiol Behav*. 1995;58:37–41.